

Theoretical Investigation on the Dynamic Characteristics of One Degree of Freedom Vibration System Equipped with Inerter of Variable Inertance

Barenten Suciu, Yoshiki Tsuji

Abstract—In this paper, a theoretical investigation on the dynamic characteristics of one degree of freedom vibration system equipped with inerter of variable inertance, is presented. Differential equation of movement was solved under proper initial conditions in the case of free undamped/damped vibration, considered in the absence/presence of the inerter in the mechanical system. Influence of inertance on the amplitude of vibration, phase angle, natural frequency, damping ratio, and logarithmic decrement was clarified. It was mainly found that the inerter decreases the natural frequency of the undamped system and also of the damped system if the damping ratio is below 0.707. On the other hand, the inerter increases the natural frequency of the damped system if the damping ratio exceeds 0.707. Results obtained in this work are useful for the adequate design of inerters.

Keywords—One degree of freedom vibration system, inerter, parallel connection, variable inertance, frequency control, damping.

I. INTRODUCTION

CONCEPT of *inertance* and its corresponding machine element, called *inerter*, was introduced by Smith in 2002, during his quest to complete the analogy between the mechanical and electrical networks [1]. Thus, in one possible analogy, one associates to the force, velocity, spring, dashpot, kinetic energy, and potential energy of the mechanical network, the current, voltage, inductor, resistor, electrical energy, and the magnetic energy of the electrical network. In such conditions, the inerter appears as corresponding to the capacitor [1].

Initially, inerter was introduced by McLaren in Formula 1 racing car suspension system, since it has the ability to generate an apparent mass (inertance) which can be considerably larger than its real mass [2]. Such feature can be materialized through various mechanisms such as: racks associated to spur gears [1], [3], ball-screw rods associated to flying-wheel ball-nuts [4], inertial hydraulic devices associated to helical tubes [2], etc.

Classical inerter is a passive element of constant inertance, which is used to provide inertial coupling, and hence, to modify the dynamic performances of the mechanical system [5]. Thus, the inerter is able to change natural frequencies of the vibration systems [5], [6], to provide nonlinear and/or apparent negative stiffness effects [7], etc. Designs with the inerter incorporated inside hydro-pneumatic dampers, or assisted by actuators in order to provide the control of the dynamic characteristics of

Barenten Suciu is with the Department of Intelligent Mechanical Engineering, Fukuoka Institute of Technology, Fukuoka, 811-0295 Japan (phone: +81-92-606-4348; fax: +81-92-606-0747; e-mail: suciu@fit.ac.jp).

Yoshiki Tsuji is with the Graduate School of Engineering, Fukuoka Institute of Technology, Fukuoka, 811-0295 Japan (e-mail: mcm15006@bene.fit.ac.jp).

the mechanical system [8], can also be found in the literature.

Inerter covers quite a large domain of applications, starting from car suspension systems [3], [9], and extending to railway suspension systems [10], [11], building suspension systems [12]-[15], cable vibration suppression devices [16], etc.

Although extensive literature was dedicated to clarifying the change of dynamical behavior due to introduction of inertance inside the mechanical systems, still the fundamental effects of the inerter addition on response to shock and vibration await further clarification. In this work, the dynamic features of one degree of freedom (1DOF) vibration system, equipped with inerter of adjustable inertance, are theoretically investigated. Adjustment range of the natural frequency is clarified, and the influence of inertance on the control sensitivity is discussed.

II. MODEL OF 1DOF VIBRATION SYSTEM EQUIPPED WITH INERTER OF VARIABLE INERTANCE

A. Case of Free Undamped Vibration

Fig. 1 shows the schematic view of the investigated 1DOF system, in the case of free undamped vibration. Concretely, the mass element m is suspended by an elastic element (spring of constant k), linked in parallel with an inerter of apparent mass, or so-called *inertance* b . Coordinate x is measured from the static equilibrium position of the mass element.

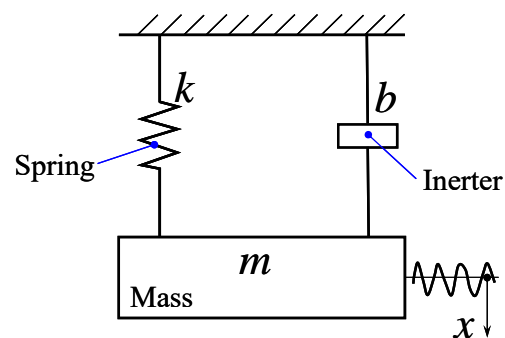


Fig. 1 Schematic view of the undamped 1DOF vibration system, in which the mass element is suspended by an elastic element connected in parallel with an inerter

A certain amount of potential energy and/or kinetic energy is supposed to be initially introduced into the system, which is then, set to free. In such circumstances, the so-called *free undamped vibration* is initiated.

For the system from Fig. 1, in the absence of the inerter, the

differential equation of movement can be written as [17]-[19]:

$$m\ddot{x} + kx = 0 \Rightarrow \ddot{x} + \omega_{n,0}^2 x = 0 \quad (1)$$

where the natural circular frequency without inerter is given by:

$$\omega_{n,0} = \sqrt{k/m} \quad (2)$$

In the presence of the inerter, the differential equation of movement can be rewritten as:

$$(m+b)\ddot{x} + kx = 0 \Rightarrow \ddot{x} + \omega_n^2 x = 0 \quad (3)$$

where the natural circular frequency with inerter is given by:

$$\omega_n = \sqrt{k/(m+b)} = \omega_{n,0} / \sqrt{1+\lambda} \quad ; \quad \lambda = b/m \geq 0 \quad (4)$$

Dimensionless inertance λ defined by (4) is regarded in this work as a variable parameter, which can be adjusted, as desired. From this standpoint, a dimensionless natural circular frequency can be defined as:

$$\Omega_n = \frac{\omega_n}{\omega_{n,0}} = \frac{1}{\sqrt{1+\lambda}} \leq 1 \Rightarrow \omega_n \leq \omega_{n,0} \quad (5)$$

From (5), one concludes that indeed the inerter is able to change ([5], [6]), and more precisely, to reduce the natural frequency of the undamped vibration system.

Next, by integrating the differential equation (1) under the following initial conditions:

$$x(t=0) = x_0 \quad ; \quad \dot{x}(t=0) = v_0 \quad (6)$$

the variation of elongation x versus time t , in the absence of the inerter, can be written as:

$$x(t) = X_0 \cos(\omega_{n,0}t - \Phi_0) \quad (7)$$

where X_0 is the amplitude:

$$X_0 = \sqrt{x_0^2 + \left(\frac{v_0}{\omega_{n,0}}\right)^2} = x_0 \sqrt{1 + \left(\frac{\omega_0}{\omega_{n,0}}\right)^2} = x_0 \sqrt{1 + \Omega_0^2} \quad (8)$$

and Φ_0 is the phase angle:

$$\Phi_0 = \tan^{-1}\left(\frac{v_0}{x_0 \omega_{n,0}}\right) = \tan^{-1}\left(\frac{\omega_0}{\omega_{n,0}}\right) = \tan^{-1} \Omega_0 \quad (9)$$

In derivation of (8)-(9), an initial equivalent circular frequency ω_0 was used, which can be defined as:

$$\omega_0 = v_0 / x_0 \in [0; \infty) \quad (10)$$

Thus, ω_0 becomes zero for nil initial velocity ($v_0 = 0$), and tends to infinity for nil initial elongation ($x_0 = 0$). Further, in derivation of (8)-(9), it appeared as convenient to define a dimensionless initial equivalent circular frequency, as:

$$\Omega_0 = \frac{\omega_0}{\omega_{n,0}} = \frac{v_0}{x_0 \omega_{n,0}} = \frac{v_0}{x_0} \sqrt{\frac{m}{k}} \in [0; \infty) \quad (11)$$

Similarly, by integrating the differential equation (3) under the same initial conditions (6), one obtains, in the presence of the inerter, the variation of elongation x versus time t as:

$$x(t) = X \cos(\omega_n t - \Phi) \quad (12)$$

where X is the amplitude:

$$X = \sqrt{x_0^2 + \left(\frac{v_0}{\omega_n}\right)^2} = x_0 \sqrt{1 + \left(\frac{\omega_0}{\omega_n}\right)^2} = x_0 \sqrt{1 + (1+\lambda)\Omega_0^2} \quad (13)$$

and Φ is the phase angle:

$$\Phi = \tan^{-1}\left(\frac{v_0}{x_0 \omega_n}\right) = \tan^{-1}\left(\frac{\omega_0}{\omega_n}\right) = \tan^{-1}(\Omega_0 \sqrt{1+\lambda}) \quad (14)$$

In order to clarify the influence of inertance on the amplitude of vibration and the phase angle, it appears as convenient to define the dimensionless amplitude as:

$$\bar{X} = \frac{X}{X_0} = \sqrt{1 + \lambda \frac{\Omega_0^2}{1 + \Omega_0^2}} \geq 1 \quad (15)$$

and the difference of phase angles as:

$$\Phi - \Phi_0 = \tan^{-1} \frac{\Omega_0(\sqrt{1+\lambda} - 1)}{\Omega_0^2 \sqrt{1+\lambda} + 1} \geq 0 \quad (16)$$

From (15)-(16), one concludes that inertance augments the amplitude and phase angle of free undamped vibration. However, it is important to observe that although the same amount of potential energy $E_{p,0} = 0.5kx_0^2$ is initially introduced into the system with and without inerter, the kinetic energy initially supplied depends on the inertance, as follows:

$$E_{k,0} = 0.5(m+b)v_0^2 = 0.5mv_0^2(1+\lambda) \quad (17)$$

Consequently, the apparent augmentation of the amplitude can be explained by the higher kinetic energy that is initially introduced into the 1DOF vibration system.

In order to quantify the effect of inertance, it is also useful to note the limits against Ω_0 of the dimensionless amplitude:

$$\lim_{\Omega_0 \rightarrow 0} \bar{X} = 1 \quad ; \quad \lim_{\Omega_0 \rightarrow \infty} \bar{X} = \sqrt{1+\lambda} \quad (18)$$

and of the difference of phase angles:

$$\lim_{\Omega_0 \rightarrow 0} (\Phi - \Phi_0) = 0 \quad ; \quad \lim_{\Omega_0 \rightarrow \infty} (\Phi - \Phi_0) = 0 \quad (19)$$

Since the partial derivatives of the dimensionless amplitude versus Ω_0 and λ are both positive:

$$\frac{\partial \bar{X}}{\partial \Omega_0} \geq 0 \quad ; \quad \frac{\partial \bar{X}}{\partial \lambda} \geq 0 \quad (20)$$

One concludes that \bar{X} monotonically increases against both the dimensionless inertance and dimensionless initial equivalent circular frequency.

Since the partial derivative of the difference of phase angles versus λ is positive:

$$\frac{\partial (\Phi - \Phi_0)}{\partial \lambda} \geq 0 \quad (21)$$

One concludes that $\Phi - \Phi_0$ monotonically augments against the dimensionless inertance. On the other hand, since the partial derivative of $\Phi - \Phi_0$ versus Ω_0 becomes nil for:

$$\Omega_{0,opt} = \frac{1}{\sqrt[4]{1+\lambda}} \quad (22)$$

a maximal value of the difference of phase angles is attained, as:

$$(\Phi - \Phi_0)_{max} = \tan^{-1} \frac{\sqrt{1+\lambda} - 1}{2\sqrt[4]{1+\lambda}} \quad (23)$$

B. Case of Free Damped Vibration

Fig. 2 shows the schematic view of the investigated 1DOF system, in the case of free damped vibration. Compared to Fig. 1, a dissipative element (dashpot of damping coefficient c), connected in parallel to the spring and inerter is added into the mechanical system.

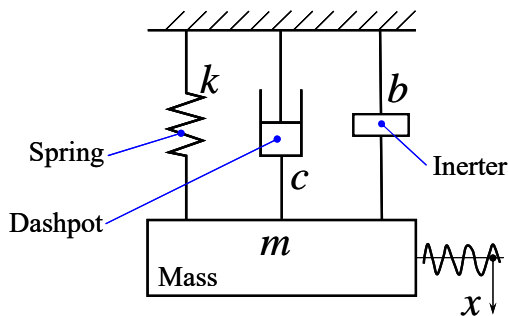


Fig. 2 Schematic view of the damped 1DOF vibration system, in which the mass element is suspended by an elastic element connected in parallel with a dissipative element and an inerter

For the system from Fig. 2, in the absence of the inerter, the

differential equation of motion can be written as [17]-[19]:

$$m\ddot{x} + c\dot{x} + kx = 0 \Rightarrow \ddot{x} + 2\zeta_0\omega_{n,0} + \omega_{n,0}^2x = 0 \quad (24)$$

where the damping ratio without inerter is given by:

$$\zeta_0 = 0.5c / \sqrt{km} \quad (25)$$

In the presence of the inerter, the differential equation of movement can be rewritten as:

$$(m+b)\ddot{x} + c\dot{x} + kx = 0 \Rightarrow \ddot{x} + 2\zeta\omega_n + \omega_n^2x = 0 \quad (26)$$

where the damping ratio with inerter is given by:

$$\zeta = 0.5c / \sqrt{k(m+b)} = \zeta_0 / \sqrt{1+\lambda} \leq \zeta_0 \quad (27)$$

It is useful to define a dimensionless damping ratio as:

$$Z = \frac{\zeta}{\zeta_0} \equiv \Omega_n = \frac{1}{\sqrt{1+\lambda}} \leq 1 \Rightarrow \zeta \leq \zeta_0 < 1 \quad (28)$$

Comparing (28) and (5), one finds that dimensionless damping ratio equals the dimensionless natural circular frequency of the undamped free vibration. Accordingly, the inerter is also able to decrease the damping ratio of the damped vibration system. Reduction rate is the same as for the natural circular frequency of the undamped vibration system (see Fig. 3).

Additionally, from (28) one observes that, if the condition to achieve vibration is satisfied by the mechanical system without inerter ($\zeta_0 < 1$), automatically it is also satisfied by the system with inerter ($\zeta < 1$).

In order to fully estimate the dissipative performances of the mechanical system, the logarithmic decrement can be defined as [17]-[19]:

$$\delta_0 = \frac{2\pi\zeta_0}{\sqrt{1-\zeta_0^2}} \quad (29)$$

in the absence of the inerter, and as:

$$\delta = \frac{2\pi\zeta}{\sqrt{1-\zeta^2}} \quad (30)$$

in the presence of the inerter. Again, it is useful to define a dimensionless logarithmic decrement, as follows:

$$\Delta = \frac{\delta}{\delta_0} = \sqrt{\frac{1-\zeta_0^2}{1-\zeta_0^2+\lambda}} \leq 1 \quad (31)$$

From (31), one concludes that the dimensionless logarithmic decrement decreases at the augmentation of the inertance.

Next, by integrating (24) under the initial conditions (6), the

variation of elongation x versus time t , in the absence of the inerter, can be written as:

$$x(t) = X_0 \cos(\omega_{d,0}t - \Phi_0) \quad (32)$$

where $\omega_{d,0}$ is the damped circular frequency:

$$\omega_{d,0} = \omega_{n,0} \sqrt{1 - \zeta_0^2} \leq \omega_{n,0} \quad (33)$$

and Φ_0 is the phase angle:

$$\Phi_0 = \tan^{-1} \left(\frac{v_0}{x_0 \omega_{d,0}} + \frac{\zeta_0}{\sqrt{1 - \zeta_0^2}} \right) = \tan^{-1} \left(\frac{\Omega_0 + \zeta_0}{\sqrt{1 - \zeta_0^2}} \right) \quad (34)$$

Similarly, by integrating (26) under the initial conditions (6), the variation of elongation x versus time t , in the presence of the inerter, can be written as:

$$x(t) = X \cos(\omega_d t - \Phi) \quad (35)$$

where ω_d is the damped circular frequency:

$$\omega_d = \omega_n \sqrt{1 - \zeta^2} \leq \omega_n \quad (36)$$

and Φ is the phase angle:

$$\Phi = \tan^{-1} \left(\frac{v_0}{x_0 \omega_d} + \frac{\zeta}{\sqrt{1 - \zeta^2}} \right) = \tan^{-1} \left(\frac{\Omega_0(1 + \lambda) + \zeta_0}{\sqrt{1 + \lambda - \zeta_0^2}} \right) \quad (37)$$

Based on (33) and (36), a dimensionless damped circular frequency can be defined as:

$$\Omega_d = \frac{\omega_d}{\omega_{d,0}} = \sqrt{\frac{1 + \lambda - \zeta_0^2}{(1 - \zeta_0^2)(1 + \lambda)^2}} \quad (38)$$

In the absence of the dashpot ($\zeta_0 = 0$), as expected, (38) reduces to $\Omega_d = \Omega_n$ (see (5) and Fig. 10). Analysis of (38) leads to the observation that $\partial \Omega_d / \partial \lambda < 0$ for $0 \leq \zeta_0 < 1/\sqrt{2}$, i.e., dimensionless damped circular frequency monotonically decreases against λ for this interval of the damping ratio (see Fig. 10). On the other hand, dimensionless damped circular frequency displays a mountain shape graph versus the dimensionless inertance for $1/\sqrt{2} \leq \zeta_0 < 1$ (Fig. 10). Since the partial derivative of Ω_d versus λ becomes nil for:

$$\lambda_{opt} = 2\zeta_0^2 - 1 \geq 0 \quad (39)$$

one finds that the maximal value of the dimensionless damped circular frequency can be calculated as follows:

$$\Omega_{d,max} = \frac{1}{2\zeta_0 \sqrt{1 - \zeta_0^2}} \quad (40)$$

Returning to the phase angle, from (34), one observes that:

$$\lim_{\Omega_0 \rightarrow 0} \Phi_0 = \tan^{-1} \frac{\zeta_0}{\sqrt{1 - \zeta_0^2}} ; \quad \lim_{\Omega_0 \rightarrow \infty} \Phi_0 = \frac{\pi}{2} \quad (41)$$

Similarly, from (37), one obtains that:

$$\lim_{\Omega_0 \rightarrow 0} \Phi = \tan^{-1} \frac{\zeta_0}{\sqrt{1 + \lambda - \zeta_0^2}} ; \quad \lim_{\Omega_0 \rightarrow \infty} \Phi = \frac{\pi}{2} \quad (42)$$

In order to clarify the influence of inertance on the phase angle, it appears as convenient to define the difference of phase angles as:

$$\Phi - \Phi_0 = \tan^{-1} \frac{f \sqrt{1 - \zeta_0^2} - g \sqrt{1 + \lambda - \zeta_0^2}}{f \cdot g + \sqrt{1 - \zeta_0^2} \cdot \sqrt{1 + \lambda - \zeta_0^2}} \quad (43)$$

where the functions f and g can be explicitly given as:

$$f(\Omega_0, \zeta_0, \lambda) = \Omega_0(1 + \lambda) + \zeta_0 ; \quad g(\Omega_0, \zeta_0) = \Omega_0 + \zeta_0 \quad (44)$$

Note that in the absence of the dashpot ($\zeta_0 = 0$), as expected, (43)-(44) reduce to (16). In order to quantify the effect of inertance, it is also useful to note the limits against Ω_0 of the difference of phase angle, as:

$$\lim_{\Omega_0 \rightarrow 0} (\Phi - \Phi_0) = \tan^{-1} \frac{\zeta_0 [\sqrt{1 - \zeta_0^2} - \sqrt{1 + \lambda - \zeta_0^2}]}{\zeta_0^2 + \sqrt{1 - \zeta_0^2} \cdot \sqrt{1 + \lambda - \zeta_0^2}} \leq 0 \quad (45)$$

and

$$\lim_{\Omega_0 \rightarrow \infty} (\Phi - \Phi_0) = 0 \quad (46)$$

Note that the results (45)-(46) are consistent with (41)-(42).

Concerning the amplitudes of vibration X_0 and X from (32) and (35), in the absence of the inerter the amplitude can be written as:

$$X_0 = x_0 \exp(-\zeta_0 \omega_{n,0} t) \sqrt{\frac{1 + 2\zeta_0 \Omega_0 + \Omega_0^2}{1 - \zeta_0^2}} \quad (47)$$

which reduces to (8), derived in the absence of the dashpot ($\zeta_0 = 0$). On the other hand, in the presence of the inerter the amplitude of vibration can be written as:

$$X = x_0 \exp\left(-\frac{\zeta_0 \omega_{n,0}}{1 + \lambda} t\right) \sqrt{\frac{1 + 2\zeta_0 \Omega_0 + (1 + \lambda) \Omega_0^2}{(1 + \lambda - \zeta_0^2)(1 + \lambda)^{-1}}} \quad (48)$$

which reduces to (13), derived in the absence of the dashpot

($\zeta_0 = 0$).

From (47)-(48), one finds, as expected, that both amplitudes X_0 and X are decreasing against the time t , but the rate of attenuation is higher in the absence of the inerter. This result can also be inferred by defining the dimensionless amplitude, as:

$$\bar{X} = \frac{X}{X_0} = \exp\left(\frac{\lambda}{1+\lambda} \zeta_0 \omega_{n,0} t\right) \sqrt{\frac{(1+\lambda)(1-\zeta_0^2) F}{1+\lambda-\zeta_0^2} G} \geq 1 \quad (49)$$

where the functions F and G can be explicitly given as:

$$\begin{cases} F(\Omega_0, \zeta_0, \lambda) = 1 + 2\zeta_0\Omega_0 + (1+\lambda)\Omega_0^2 \\ G(\Omega_0, \zeta_0) = 1 + 2\zeta_0\Omega_0 + \Omega_0^2 \end{cases} \quad (50)$$

Thus, X appears to be larger than X_0 due to the positive exponent $\zeta_0 \omega_{n,0} \lambda / (1+\lambda) \geq 0$ that multiplies the time t under the exponential function of (49).

III. RESULTS AND DISCUSSIONS

A. Case of Free Undamped Vibration

Fig. 3 illustrates the variation of the dimensionless natural circular frequency versus the dimensionless inertance. As already discussed in relation with (5), the inerter decreases the natural frequency of the free undamped vibration system. This result agrees with the previously reported findings by [5], [6].

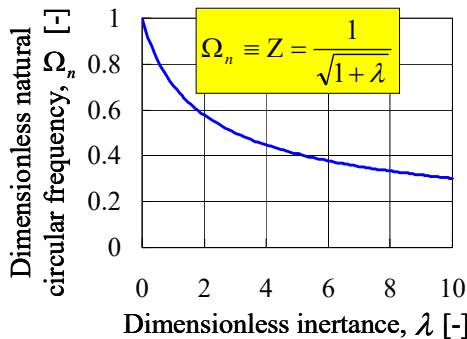


Fig. 3 Variation of the dimensionless natural circular frequency versus the dimensionless inertance

Fig. 4 presents the variation of the dimensionless amplitude versus the dimensionless inertance, for various values of the dimensionless initial equivalent circular frequency $\Omega_0 = 0, 1, 2, 3, 10$, and infinity. As found in relation with (15), (18) and (20), the dimensionless amplitude increases versus the dimensionless inertance and also versus the dimensionless initial equivalent circular frequency. Rate of increase is higher for lower values of Ω_0 (see the rate of increase from 0 to 1), and lower for larger values of Ω_0 (see the rate of increase from 10 to infinity).

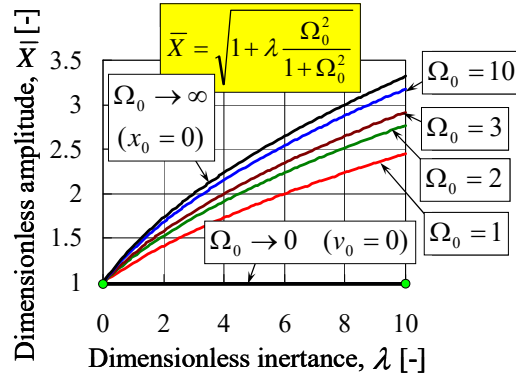


Fig. 4 Variation of the dimensionless amplitude versus the dimensionless inertance, for various values of the dimensionless initial equivalent circular frequency

Fig. 5 shows the variation of the difference of phase angle versus the dimensionless inertance, for various values of the dimensionless initial equivalent circular frequency $\Omega_0 = 0, 1, 2, 3, 10$, and infinity. As mentioned in relation with (16), (19), and (21), regardless the value of Ω_0 , the phase difference $\Phi - \Phi_0$ monotonically increases against the dimensionless inertance.

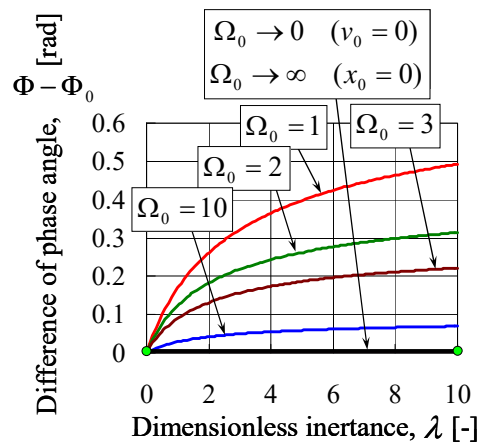


Fig. 5 Variation of the difference of phase angle versus the dimensionless inertance, for various values of the dimensionless initial equivalent circular frequency

Fig. 6 illustrates the variation of the difference of phase angle versus the dimensionless initial equivalent circular frequency, for various values of the dimensionless inertance $\lambda = 0.5, 1, 2, 3$, and 10. Difference of phase angle displays a mountain shape graph versus the dimensionless initial equivalent circular frequency. Height of the mountain peak increases versus the dimensionless inertance (see (23) and Figs. 6, 8). Position of the mountain peak is given by the optimal value of the initial equivalent circular frequency (see (22) and Figs. 6, 7). Location of the mountain peak tends to shift toward lower equivalent circular frequencies at augmentation of the dimensionless inertance (Figs. 6, 7).

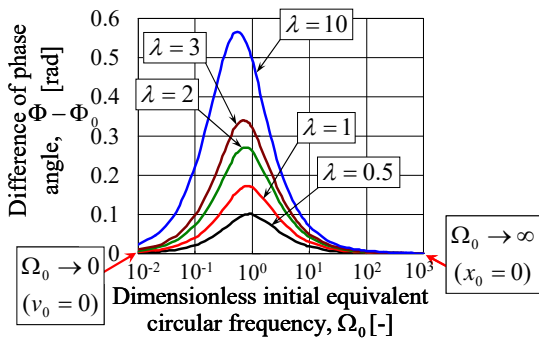


Fig. 6 Variation of the difference of phase angle versus the dimensionless initial equivalent circular frequency, for various values of the dimensionless inertia

Fig. 7 shows the monotonical reduction of the optimal value of the dimensionless initial equivalent circular frequency against the dimensionless inertia. Fig. 8 shows the variation (monotonical augmentation) of the maximal value of the difference of phase angle versus the dimensionless inertia.

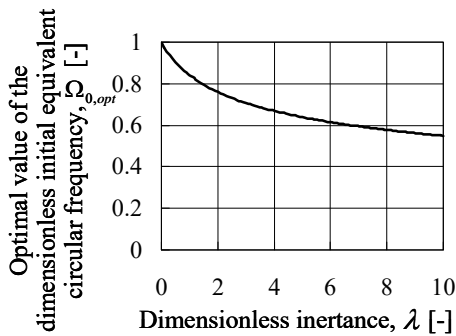


Fig. 7 Variation of the optimal value of the dimensionless initial equivalent circular frequency versus the dimensionless inertia

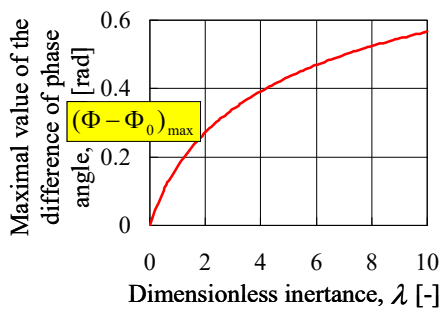


Fig. 8 Variation of the maximal value of the difference of phase angle versus the dimensionless inertia

B. Case of Free Damped Vibration

Fig. 9 shows the variation of the dimensionless logarithmic decrement versus the dimensionless inertia, for various values of the damping ratio $\zeta_0 = 0, 0.35, 0.5, 0.707, 0.8, 0.9,$ and 0.99 . As noticed in connection with (31), the dimensionless

logarithmic decrement decreases at the augmentation of the dimensionless inertia. Rate of reduction is higher for larger values of the damping ratio.

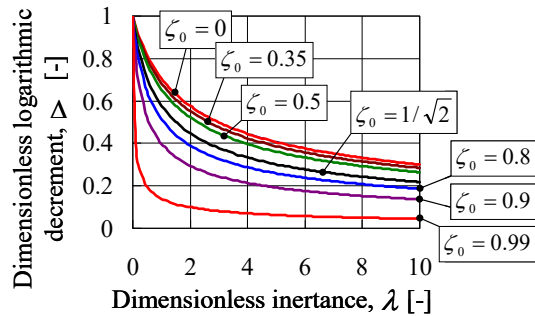


Fig. 9 Variation of the dimensionless logarithmic decrement versus the dimensionless inertia, for various values of the damping ratio

Fig. 10 presents the variation of the dimensionless damped circular frequency versus the dimensionless inertia, for various values of the damping ratio $\zeta_0 = 0, 0.55, 0.707, 0.8, 0.9, 0.95, 0.98,$ and 0.99 . As discussed in connection with (38), for $0 \leq \zeta_0 < 1/\sqrt{2}$, the dimensionless damped circular frequency monotonically decreases against the dimensionless inertia. On the other hand, for $1/\sqrt{2} \leq \zeta_0 < 1$, a mountain shape graph is obtained versus the dimensionless inertia. Height of the peak increases versus ζ_0 (see (40) and Figs. 10, 12). Position of the peak is given by the optimal value of the inertia (see (39) and Figs. 10, 11). Location of the mountain peak tends to shift toward higher values of the dimensionless inertia at augmentation of the damping ratio ζ_0 (see Figs. 10-12).

Fig. 11 shows the variation (monotonical augmentation) of the optimal dimensionless inertia versus the damping ratio.

Fig. 12 presents the variation (monotonical augmentation) of the maximal value of the dimensionless damped circular frequency versus the damping ratio.

Next, Fig. 13 is added in order to discuss the significance of the results shown by Fig. 10.

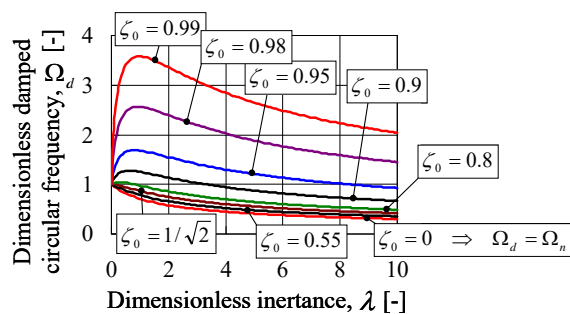


Fig. 10 Change of the dimensionless damped circular frequency versus the dimensionless inertia, for various values of the damping ratio

Compared to Fig. 10, the right side of Fig. 13 presents the change of vibration frequency by adjusting the dimensionless

inertance, only for $\zeta_0 = 0.99$. For instance, by changing the inertance from $\lambda = 1$ (reference vibration) to $\lambda_{opt} = 0.96$ (fastest vibration), a 3.6 times augmentation of the frequency can be achieved. Further, by increasing the inertance from λ_{opt} to $\lambda = 10$ (faster vibration), the frequency can now be reduced to a value of twice the frequency of the reference vibration.

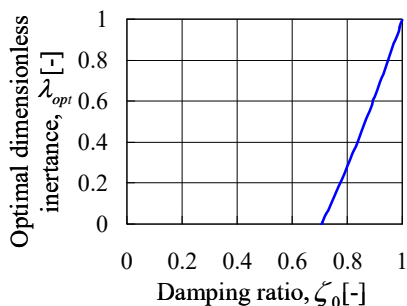


Fig. 11 Variation of the optimal dimensionless inertance versus the damping ratio

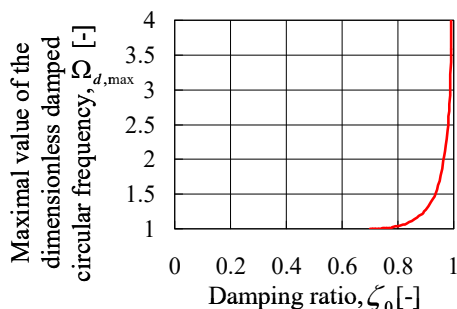


Fig. 12 Variation of the maximal value of the dimensionless damped circular frequency versus the damping ratio

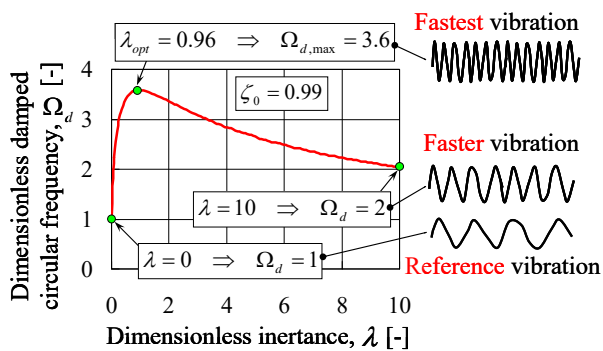


Fig. 13 Control of the damped circular frequency of the mechanical system by employing an inerter of adjustable inertance

In conclusion, Fig. 13 proves the possibility to control the damped circular frequency of the mechanical system by employing an inerter of adjustable inertance. Since the range of adjustment and the control sensitivity are larger for $\lambda \in [0; \lambda_{opt}]$, this interval of variation for inertance seems to be preferable.

Variation of the difference of the phase angle versus the

dimensionless initial equivalent circular frequency, for various values of the dimensionless inertance ($\lambda = 0.5, 1, 2, 3$, and 10), is shown in Fig. 14 for $\zeta_0 = 0.25$, in Fig. 15 for $\zeta_0 = 0.5$, in Fig. 16 for $\zeta_0 = 0.75$, and in Fig. 17 for $\zeta_0 = 1$. Figs. 14-17 should be regarded in correlation with Fig. 6, constructed for the undamped vibration system, i.e., for $\zeta_0 = 0$. One observes that, for $\zeta_0 = 0$, the difference of phase angle is positive, regardless the values of the inertance (Fig. 6). On the contrary, for $\zeta_0 = 1$ the difference of phase angle becomes negative, regardless the values of the inertance (Fig. 14). As expected, for intermediate values of the damping ratio ($\zeta_0 = 0.25, 0.5$, and 0.75), the shape of the graphs gradually changes from the mountain like shape observed for $\zeta_0 = 0$ to monotonically increasing shape noticed for $\zeta_0 = 1$. From Figs. 14-17, one concludes that the variation pattern of $\Phi - \Phi_0$ is relatively complex, due to the superposed influence of three parameters ($\zeta_0, \lambda, \Omega_0$). However, it was generally observed that the inertance increases the absolute value of the difference of phase angle.

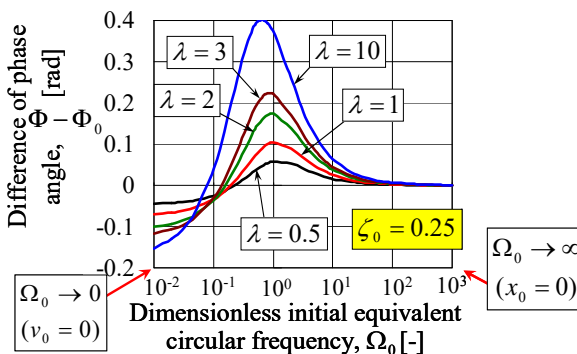


Fig. 14 Variation of the difference of phase angle versus the dimensionless initial equivalent circular frequency, for various values of the dimensionless inertance and $\zeta_0 = 0.25$

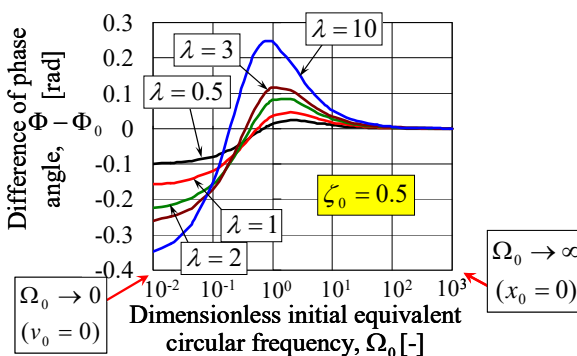


Fig. 15 Variation of the difference of phase angle versus the dimensionless initial equivalent circular frequency, for various values of the dimensionless inertance and $\zeta_0 = 0.5$

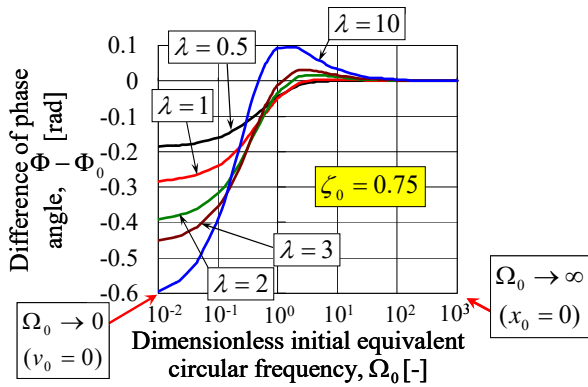


Fig. 16 Variation of the difference of phase angle versus the dimensionless initial equivalent circular frequency, for various values of the dimensionless inertance and $\zeta_0 = 0.75$

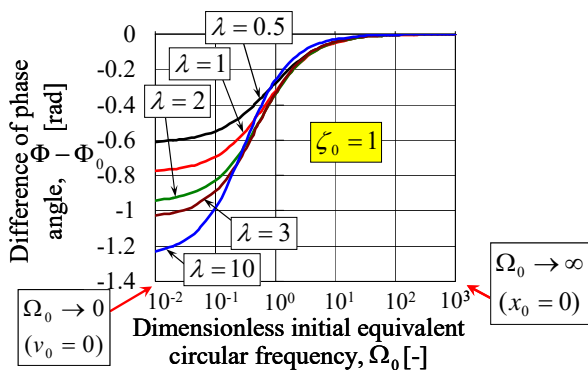


Fig. 17 Variation of the difference of phase angle versus the dimensionless initial equivalent circular frequency, for various values of the dimensionless inertance and $\zeta_0 = 1$

IV. CONCLUSIONS

From the theoretical investigation of the proposed 1DOF vibration system supplied with inerter of changeable inertance, the following conclusions can be drawn:

A. Case of Free Undamped Vibration

- 1) Inerter decreases the natural frequency of the undamped vibration system.
- 2) Inerter increases the amplitude and phase angle of the system. Augmentation of amplitude is produced by the higher kinetic energy, which is initially supplied into the system.
- 3) Amplitude increases versus both the dimensionless inertance and the dimensionless initial equivalent circular frequency.
- 4) Phase angle increases against the dimensionless inertance. On the other hand, the difference of phase angle displays a mountain shape graph versus the dimensionless initial equivalent circular frequency. Height of the mountain peak increases versus the dimensionless inertance. Position of the mountain peak appears shifted toward lower equivalent

circular frequencies at augmentation of the dimensionless inertance.

B. Case of Free Damped Vibration

- 5) Inerter reduces the damping ratio of the vibration system. Reduction rate is the same as for the natural circular frequency of the undamped vibration system.
- 6) If the condition of achieving vibration is satisfied by the system without inerter, automatically it is also satisfied by the system with inerter.
- 7) Inerter reduces the logarithmic decrement of the system. This reduction effect is more prominent for larger damping ratios of the mechanical system.
- 8) One proved the possibility to control the natural damped frequency of the mechanical system by using an inerter of adjustable inertance. For damping ratios smaller than 0.707, inertance reduces the frequency. For damping ratios larger than 0.707, inertance increases the frequency in a relatively steep manner, up to a maximal value, which corresponds to the optimal inertance. Further augmentation of the inertance leads to the frequency reduction, in a relatively slow manner. Range of adjustment and the control sensitivity are larger for values of the inertance below the optimal inertance.
- 9) Inerter increases the amplitude of damped vibration system, too. Again, this effect is generated by the larger kinetic energy initially furnished to the mechanical system.
- 10) Inertance increases the absolute value of the difference of phase angle.

REFERENCES

- [1] M.C. Smith, "Synthesis of Mechanical Networks: The Inerter", *IEEE Transactions on Automatic Control*, 47(10), pp. 1648–1662, 2002.
- [2] I.F. Lazar, S.A. Neild, and D.J. Wagg, "Design and Performance Analysis of Inerter-Based Vibration Control Systems", *Proc. of IMAC XXXII Conference and Exposition on Structural Dynamics*, pp. 1–7, 2014.
- [3] M.C. Smith, and F.C. Wang, "Performance Benefits in Passive Vehicle Suspensions Employing Inerters", *Vehicle System Dynamics*, 42(4), pp. 235–257, 2004.
- [4] Y. Shen, L. Chen, X. Yang, D. Shi, and J. Yang, "Improved Design of Dynamic Vibration Absorber by Using the Inerter and its Application in Vehicle Suspension", *Journal of Sound and Vibration*, 369(1), pp. 148–158, 2016.
- [5] J. Yang, "Force Transmissibility and Vibration Power Flow Behaviour of Inerter-Based Vibration Isolators", *Journal of Physics: Conference Series* 744(012234), pp. 1–8, 2016.
- [6] M.Z.Q. Chen, Y. Hu, L. Huang, and G. Chen, "Influence of Inerter on Natural Frequencies of Vibration Systems", *Journal of Sound and Vibration*, 333(7), pp. 1874–1887, 2014.
- [7] J. Yang, Y.P. Xiong, and J.T. Xing, "Dynamics and Power Flow Behaviour of a Nonlinear Vibration Isolation System with a Negative Stiffness Mechanism", *Journal of Sound and Vibration*, 332(1), pp. 167–183, 2013.
- [8] M. Zilletti, "Feedback Control Unit with an Inerter Proof-Mass Electrodynamic Actuator", *Journal of Sound and Vibration*, 369(1), pp. 16–28, 2016.
- [9] Y. Hu, M.Z.Q. Chen, and Z. Shu, "Passive Vehicle Suspensions Employing Inerters with Multiple Performance Requirements", *Journal of Sound and Vibration*, 333(8), pp. 2212–2225, 2014.
- [10] J.Z. Jiang, A.Z. Matamoros-Sanchez, R.M. Goodall, and M.C. Smith, "Passive Suspensions Incorporating Inerters for Railway Vehicles", *Vehicle System Dynamics*, 50 Supplement, pp. 263–276, 2012.
- [11] F.C. Wang, M.K. Liao, B.H. Liao, H.J. Sue, and H.A. Chan, "The Performance Improvements of Train Suspension Systems with

- Mechanical Networks Employing Inerters”, *Vehicle System Dynamics*, 47(7), pp. 805–830, 2009.
- [12] F.C. Wang, M.F. Hong, and C.W. Chen, “Building Suspensions with Inerters”, *PI Mechanical Engineering C*, 224 (8), pp. 1605–1616, 2010.
- [13] F.C. Wang, C.W. Chen, M.K. Liao, and M.F. Hong, “Performance Analyses of Building Suspension Control with Inerters”, *Proc. of 46th IEEE Conference on Decision and Control*, 4434186, pp. 3786–3791, 2007.
- [14] K. Ikago, K. Saito, and N. Inoue, “Seismic Control of Single-Degree-of-Freedom Structure using Tuned Viscous Mass Damper”, *Earthquake Engineering and Structural Dynamics*, 41(3), pp. 453–474, 2012.
- [15] I.F. Lazar, S.A. Neild, and D.J. Wagg, “Using an Inerter-Based Device for Structural Vibration Suppression”, *Earthquake Engineering and Structural Dynamics*, 43(8), pp. 1129–1147, 2014.
- [16] I.F. Lazar, S.A. Neild, and D.J. Wagg, “Performance Analysis of Cables with Attached Tuned-Inerter- Dampers”, *Proc. of 33rd IMAC Dynamics of Civil Structures*, 2, pp. 433–441, 2015.
- [17] J.P. Den Hartog, *Mechanical Vibrations*. London: McGraw-Hill, 1940.
- [18] D.J. Inman, and R.J. Singh, *Engineering Vibration*. New York: Prentice Hall, 2001.
- [19] H. Benaroya, and M.L. Nagurka, *Mechanical Vibration: Analysis, Uncertainties, and Control*. London: CRC Press, 3rd ed., 2010.

Barenten Suciu was born on July 9, 1967. He received Dr. Eng. Degrees in the field of Mech. Eng. from the Polytechnic University of Bucharest, in 1997, and from the Kobe University, in 2003. He is working as Professor at the Department of Intelligent Mech. Eng., Fukuoka Institute of Technology. He is also entrusted with the function of Director of the Electronics Research Institute, affiliated to the Fukuoka Institute of Technology. He is member of JSME and JSAE. His major field of study is the tribological and dynamical design of various machine elements.

Yoshiki Tsuji was born on October 28, 1992. He received the Eng. Degree from Fukuoka Institute of Technology, in 2014. He is a master-course student at the Graduate School of Engineering, Fukuoka Institute of Technology. His research interests are in the field of vibration absorbers for vehicle suspensions.